Very-long-period volcanic earthquakes beneath Mammoth Mountain, California

David P. Hill, Phillip Dawson, Malcolm J. S. Johnston, and A. M. Pitt
U.S. Geological Survey, Menlo Park, CA, USA

Glenn Biasi and Ken Smith
University of Nevada, Reno, NV, USA

Received 31 January 2002; revised 1 April 2002; accepted 8 April 2002; published 17 May 2002.

[1] Detection of three very-long-period (VLP) volcanic earthquakes beneath Mammoth Mountain emphasizes that magmatic processes continue to be active beneath this young, eastern California volcano. These VLP earthquakes, which occurred in October 1996 and July and August 2000, appear as bell-shaped pulses with durations of one to two minutes on a nearby borehole dilatometer and on the displacement seismogram from a nearby broadband seismometer. They are accompanied by rapid-fire sequences of high-frequency (HF) earthquakes and several long-period (LP) volcanic earthquakes. The limited VLP data are consistent with a CLVD source at a depth of ~3 km beneath the summit, which we interpret as resulting from a slug of fluid (CO_2–saturated magmatic brine or perhaps basaltic magma) moving into a crack. *INDEX TERMS:* 7280 Seismology: Volcano seismology; (8419); 8434 Volcanology: Magma migration; 8499 Volcanology: General or miscellaneous; 8419 Volcanology: Eruption monitoring (7280)

1. Introduction

[2] As the number of volcanic systems monitored with broadband instrumentation increases, it is becoming increasingly clear that very-long-period (VLP) volcanic earthquakes (sources that generate seismic waves with dominant periods between ~2 and ~100 seconds [*Kumagai et al.*, 2001; *Ohiminato et al.*, 1998]), represent an important component of the spectrum of geophysical signals produced by active magmatic processes. In this paper, we describe three VLP earthquakes that have occurred beneath Mammoth Mountain in eastern California: one in 1996 and two in 2000.

[3] Mammoth Mountain is a young cumulo-volcano on the southwest rim of Long Valley caldera that formed in a series of dome-building eruptions between 100,000 and 50,000 years before present (ybp) [Figure 1, *Bailey et al.*, 1976; *Mahood et al.*, 2000]. Volcanic unrest beneath Mammoth Mountain since 1980 has included (1) occasional swarms of small ($M \leq 3$), shallow ($z \leq 10$ km), high-frequency (HF) earthquakes (or volcano-tectonic (VT) earthquakes), (2) mid-crustal, long-period (LP) volcanic earthquakes (dominant periods ~1 to 0.2 sec and depths from 10 km to 25 km), and (3) diffuse emission of magmatic carbon dioxide (CO_2). The mid-crustal LP earthquakes and CO_2 emissions began following an 8-month-long swarm and dike intrusion in 1989 [*Farrar et al.*, 1995; *Hill*, 1996; *Pitt and Hill*, 1994]. This swarm included many spasmodic bursts (rapid-fire sequences of HF earthquakes that persisted for minutes to tens of minutes). Spasmodic bursts are thought to result from cascading sequences of both double-couple, shear failures [*Hill et al.*, 1990] and hydrofractures.

0094-8276/02/2002GL014833$05.00

2. VLP Earthquakes

[4] The three VLP earthquakes described here represent a third class of Mammoth Mountain earthquake. The first occurred in July 1996 and the other two in July and August 2000 (VLP's #1, #2, and #3 in Table 1, respectively). All three appear as quasi-symmetric, bell-shaped, dilatational strain transients with durations ranging from 50 to 115 sec and peak amplitudes of ~ 1 nanostrain as recorded in the seismic band of the POPA borehole dilatometer located 4 km west of Mammoth Mountain (Figure 2a). VLP #3 was also recorded by a CMG-3 broadband seismometer, which was installed on 13 July 2000 in a mine adit (station OMM) located 4 km SE of Mammoth Mountain. The three displacement components on OMM for VLP#3 represent a single pulse down to the NW with an amplitude of ~10 micrometers and duration between 30 to 50 sec (Figure 2c).

[5] Although all three VLP strain transients on POPA have grossly similar forms, there remain notable differences (Figure 2a). The ~114 sec duration of VLP #2, for example, is roughly twice that of VLP #3. Both VLP's #1 and #3 are solitary while a second,

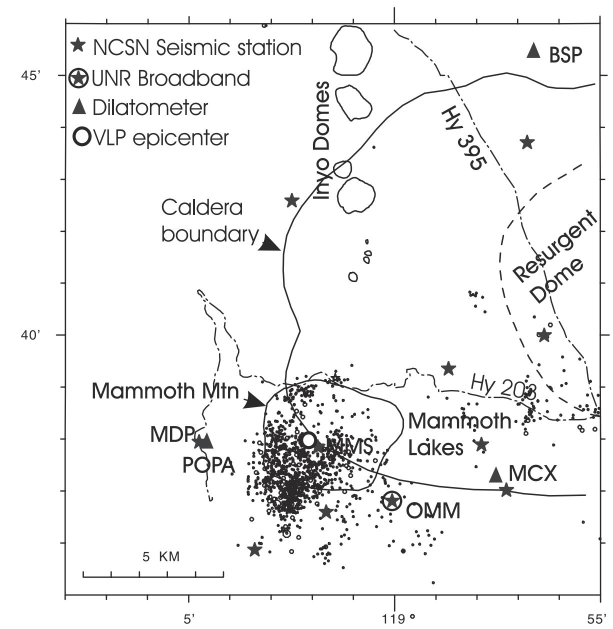

Figure 1. Map of Mammoth Mountain and the western half of Long Valley caldera showing station locations. Small circles are epicentral locations for earthquakes of the 1989 earthquake swarm. Large open circle is inferred location for the LVP earthquakes.

Table 1. Parameters for the Mammoth Mountain VLP Earthquakes

VLP earthquakes			Dilatational strain (nanostrain, extension +)				OMM displacements (micrometers)		
Number	Date	Time(UT)	POPA	POPA(static)	MCX(static)	BSP(static)	N(+)	E(+)	Z(+)
#1	13/10/96	21:43	1.0	0.07	–	–	–	–	–
#2	06/07/00	03:56	1.0	0.8	0.4	−0.2	–	–	–
#3	13/08/00	03:00	1.2	<0.05	<0.05	<0.05	6.2	−5.7	5.0
#3	CLVD: calculated		1.2	–	–	–	7.4	−5.9	6.9

Station locations are in Figure 1. Polarities and amplitudes from traces plotted in Figure 2. Dilatometers MCX and BSP, which began operation in mid-1999, were recording just one sample per 10 minutes through the summer of 2000, and the data were too strongly aliased to resolve the strain transients for VLP's #2 and #3. Calculated polarities and amplitudes for VLP #3 for a CLVD source at (37° 37.8′ N, −119° 01.8′ W, z ~ 3 km) with T-axis trending N 70° E and a scalar moment, $M_0 \sim 1.3 \times 10^{14}$ Nm.

smaller VLP earthquake follows VLP #2 by roughly 100 sec. VLP's #1 and #2 produced detectable static offsets while #3 did not (Table 1). The onset of each of the VLP's is accompanied by the onset of higher frequency energy in the form of spasmodic bursts, the duration and intensity of which varies from one VLP to the next (Figures 2a and 2b). In addition, VLP's #1 and #2 are accompanied by LP earthquakes (see Figure 3).

[6] The limited instrumental records for the VLP earthquakes leaves their source parameters poorly resolved. To gain insight into plausible source models for the VLP earthquakes consistent with available data, we assume: (1) the VLP earthquakes and the associated HF and LP earthquakes are spatially proximal, and (2) the VLP earthquakes are similar events with nearly coincident hypocenters. The latter assumption is consistent with the similar form of all three strain transients on POPA (Figure 2a).

[7] Hypocentral locations for HF earthquakes within spasmodic bursts accompanying the VLP earthquakes occupy a volume about 5 km in diameter centered at a depth of 3 km beneath the summit of Mammoth Mountain (Figure 4). A location for VLP #3 within this volume is supported by the rectilinear particle motion on the

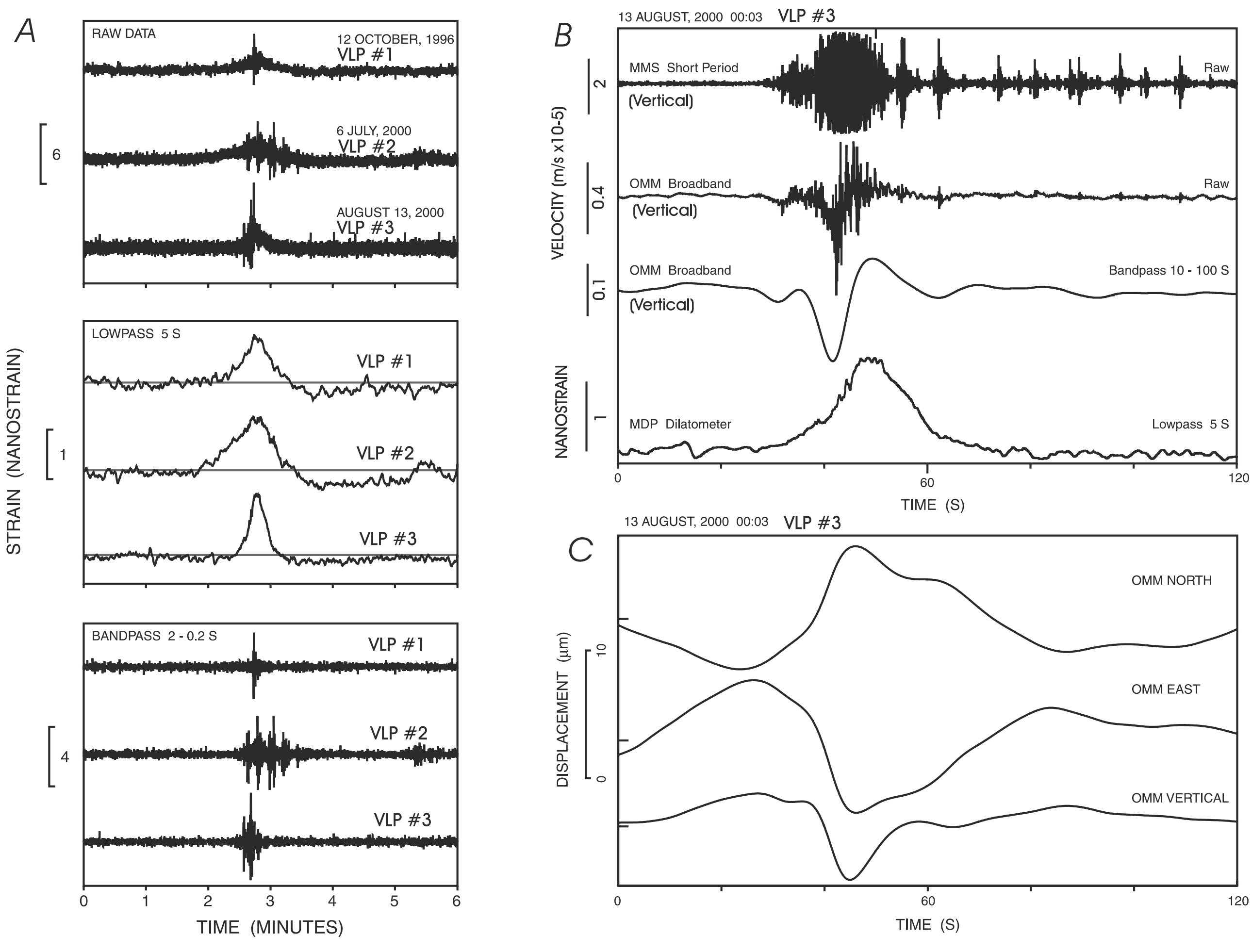

Figure 2. Waveforms for the VLP earthquakes. (A) Dilatational strain transients on the seismic band (400 to 0.1 sec) of the POPA borehole dilatometer. Extension is positive. (B) VLP #3 on (1) the NCSN short-period (1 sec) station MMS, (2) the vertical velocity component of broadband at OMM (unfiltered and filtered with a 10- to 100-sec band pass), and (3) POPA with a high-cut filter at 5 sec (same as in 2A). (C) Displacement seismograms VLP #3 for the OMM broadband station. Times scale same as for *B*.

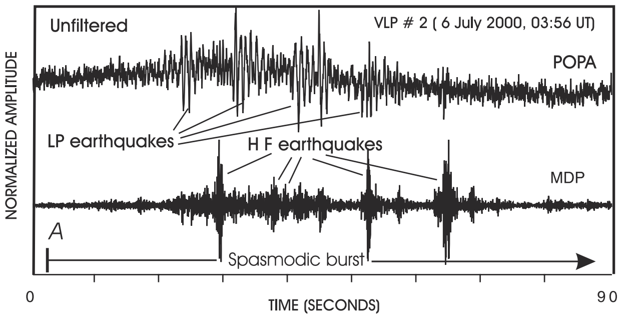

Figure 3. Details of VLP #2 illustrating the associated long-period (LP) earthquakes and the spasmodic burst of rapid-fire HF earthquakes as recorded on the seismic band of the POPA borehole dilatometer and the adjacent short-period, vertical-component seismometer (MDP).

broadband station, OMM, which defines a line dipping roughly 30° to the northwest passing beneath Mammoth Mountain at depths of 2 to 3 km (Figure 4).

[8] In a limited, forward-modeling search over point-source dislocation models beneath Mammoth Mountain, we find that a compensated linear-vector dipole (CLVD) at a depth of 3 km comes close to matching the phase and peak amplitudes for POPA and OMM for VLP #3 transient (Table 1, Figure 4). This source has a scalar moment of $M_0 \sim 1.3 \times 10^{14}$ Nm with its major dipole (T axis) trending N 70° W. Stations POPA and OMM are within the near field for a slowly evolving VLP source at this location, and we assume that quasi-static strains and displacements computed for an elastic half-space [*Okada*, 1985] provide an adequate approximation to near-field peak amplitudes and phases. Our search is far from exhaustive, however, and with available data limited to at most four components (one dilatational strain and three displacement components for VLP #3), this model is hardly unique. At this stage, we claim only that this provisional CLVD source model is consistent with the limited available data and that it is physically and geologically reasonable. The test will come with future VLP earthquakes recorded on additional, well-placed broadband instruments.

3. Discussion

[9] The VLP earthquakes beneath Mammoth Mountain are part of a composite sequence consisting of (1) a slowly evolving VLP source process that develops over a period of one to two minutes, (2) spasmodic bursts of HF earthquakes, and (3) occasional LP volcanic earthquakes, which we assume to be all co-located in the same general crustal volume. A provisional model consistent with the strain and displacement data for VLP #3 involves a CLVD source located at a depth of ~3 km directly beneath the summit of Mammoth Mountain. Its epicenter is near the intersection of the 1989 dike intrusion and the caldera boundary (Figure 4). The N 20° W strike of symmetry plane (crack orientation) for this CLVD is subparallel with the local strike of the caldera boundary beneath Mammoth Mountain and may represent opening along this inherited plane of weakness. By analogy with similar VLP earthquakes beneath Kilauea Volcano [*Ohiminato et al.*, 1998], we interpret the CLVD source as reflecting the transport of a slug of relatively invicid fluid (CO_2-saturated magmatic brine or perhaps basaltic magma) from a near-by isotropic volume into a vertical crack. This model involves local mass transfer with no net volume change over the source volume consistent with the absence of a static offset in dilatational strain for VLP #3. The scalar moment for the CLVD of $\sim 1.3 \times 10^{14}$ Nm (the equivalent of a M~3 earthquake) suggests the volume, ΔV, of fluid transported is on the order of 3×10^3 m^3 (using Mo = $(4/3)\mu\ \Delta V$ for a CLVD, where μ is the shear modulus, [*Julian*, 1983]).

[10] We interpret the associated spasmodic bursts and LP earthquakes as a response to transient changes in strain [*Dieterich et al.*, 2000] and pore pressure in the brittle crust adjacent to the VLP

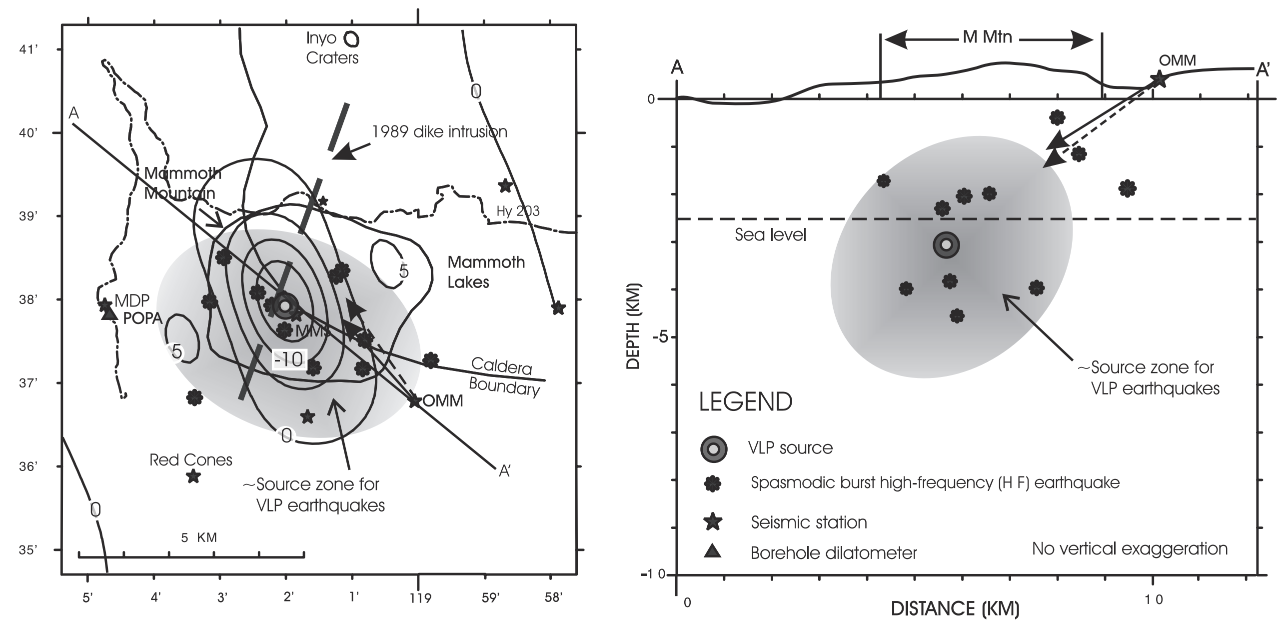

Figure 4. Source zone (shaded ellipse) and locations for spasmodic-burst HF earthquakes and the CLVD source model for VLP #3 in map view and cross-section, (A-A′). Heavy dashed line is location of dike intruded beneath Mammoth Mountain during the 1989 swarm. Heavy line in section A-A′ is topographic profile. Contours are dilatational strain for the CLVD source (contour interval: 5 nanostrain). Solid and dashed vectors from station OMM compare observed and calculated peak displacements, respectively, for VLP #3 from Table 1.

source. The rapid-fire sequence of HF earthquakes comprising a spasmodic burst represents cascading, coupled shear failures and hydrofractures in a fracture mesh [*Sibson*, 1986] surrounding the VLP source. Spasmodic bursts were common during the 1989 Mammoth Mountain earthquake swarm, and their close association with the VLP earthquakes described here suggests that VLP earthquakes were probably common during the 1989 swarm as well (no instrumentation was in place at the time capable of detecting VLP earthquakes). We suppose that the associated LP earthquakes result from resonance within cracks filled by a frothy (bubbly) fluid [*Chouet*, 1992] or a non-linear fluid-wall rock interaction as the fluid moves through a constriction in the conduit walls [*Julian*, 1994].

4. Conclusions

[11] The occurrence of these three VLP volcanic earthquakes is a reminder that magmatic processes continue to be active at relatively shallow depths (3 to 5 km) beneath Mammoth Mountain. The occurrence of only three such events over the last six years, however, does not constitute evidence for escalation in magmatic activity or an impending volcanic eruption.

[12] **Acknowledgments.** We are grateful to Rachael Abercrombie, Bernard Chouet, and Bruce Julian and two anonymous reviewers for their constructive comments on this manuscript. We also thank the Keck Foundation for support to UNR for station OMM. USGS External Grant 01HQAG0009 supported UNR seismic network operations.

References

Bailey, R. A., G. B. Dalrymple, and M. A. Lanphere, Volcanism, structure, and geochronology of Long Valley Caldera, Mono County, California, *Journal of Geophysical Research*, *81*(5), 725–744, 1976.

Chouet, B., A seismic model for the source of long-period events and harmonic tremor, in *Volcanic Seismology*, edited by P. Gasparini, R. Scarpa, and K. Aki, pp. 133–156, Springer-Verlag, Berlin, Heidelberg, New York, 1992.

Dieterich, J., V. Cayol, and P. Okubo, The use of earthquake rate changes as a stress meter at Kilauea volcano, *Nature*, *408*, 457–460, 2000.

Farrar, C. D., M. L. Sorey, W. C. Evans, J. F. Howle, B. D. Kerr, B. M. Kennedy, C.-Y. King, and J. R. Southon, Forest-killing diffuse CO_2 emission at Mammoth Mountain as a sign of magmatic unrest, *Nature*, *376*(6542), 675–678, 1995.

Hill, D. P., Earthquakes and carbon dioxide beneath Mammoth Mountain, California, *Seismological Research Letters*, *67*(1), 8–15, 1996.

Hill, D. P., W. L. Ellsworth, M. J. S. Johnston, J. O. Langbein, D. H. Oppenheimer, A. M. Pitt, P. A. Reasenberg, M. L. Sorey, and S. R. McNutt, The 1989 earthquake swarm beneath Mammoth Mountain, California; an initial look at the 4 May through 30 September activity, *Bulletin of the Seismological Society of America*, *80*(2), 325–339, 1990.

Julian, B. R., Evidence for dyke intrusion earthquake mechanisms near Long Valley Caldera, California, *Nature*, *303*, 323–325, 1983.

Julian, B. R., Volcanic tremor: nonlinear excitation by fluid flow, *Journal of Geophysical Research*, *99*(B6), 11,859–11,877, 1994.

Kumagai, H., T. Ohminato, M. Nakano, M. Ool, A. Kubo, H. Inoue, and J. Oikawa, Very-long-period seismic signals and caldera formation at Miayake Island, Japan, *Science*, *293*, 687–690, 2001.

Mahood, G., J. H. Ring, and M. McWilliams, Contemporaneous mafic and silicic eruptions during the past 160 ka at Long Valley caldera, Californai: implications of new 40Ar/39Ar eruption ages for current volcanic hazards, *EOS, Transactions, American Geophysical Union*, *81*(48), F1321, 2000.

Ohiminato, T., B. A. Chouet, P. B. Dawson, and S. Kedar, Waveform inversion of very-long-period impulsive signals associated with magmatic injection beneath Kilauea volcano, Hawaii, *Journal of Geophysical Research*, *103*, 23,839–23,862, 1998.

Okada, Y., Surface deformation due to shear and tensile faults in a half-space, *Bulletin of the Seismological Society of America*, *75*, 1135–1154, 1985.

Pitt, A. M., and D. P. Hill, Long-period earthquakes in the Long Valley Caldera region, eastern California, *Geophysical Research Letters*, *21*(16), 1679–1682, 1994.

Sibson, R. H., Structural permeability of fluid-driven fault-fracture meshes, *Journal of Structural Geology*, *18*, 1031–1042, 1986.

D. P. Hill, P. Dawson, M. J. S. Johnston, and A. M. Pitt, U.S. Geological Survey, Menlo Park, CA 94025, USA.

G. Biasi and K. Smith, University of Nevada, Reno, NV 89557, USA.